Static Structural Analysis and Determination of Low-Cost Component Sizes of The Paper Pulper Machines

Static Structural Analysis and Determination of Low-Cost Component Sizes of The Paper Pulper Machines

Kriswanto[1], Supraptono[1], A Roziqin[1], F Hasyim[1], D D Saputro[1], and B Wijayanto[2]

[1]Department of Mechanical Engineering, Universitas Negeri Semarang, Gd E9 Kampus Sekaran Gunungpati, Semarang, Indonesia
[2] Balai Pengembangan Teknologi Logam dan Kayu (BPTLK) Dinas Perindustrian dan Perdagangan Provinsi Jawa Tengah, Muktiharjo Lor, Semarang, Indonesia

kriswanto@mail.unnes.ac.id

Abstract. Paper pulper machines a capacity of 83 litres/process must have a low-cost material, robust and safe to operate. Paper pulper machine components analysed are tubes, frames, helical screw shaft and the shaft holder. The method uses a static structural analysis to obtain von mises stress and displacement. Static structural analysis uses finite element analysis with the help of CATIA® Software. The safe component size and lowest cost (safety factor more than 2.5) were selected in this study. Calculation of costs by multiplying the size of the material needs by material prices. Tube components use SUS 304 with thickness variations of 0.5, 0.6, 0.8, 1, 1.5, and 2mm. Frame and shaft holder using L shape ASTM A36 size 40x40mm and 50 x50 mm with thickness variations of 3, 4, and 5 mm respectively. Variations in material size are determined based on standard material sizes available on the market. The simulation result of each component shows the thicker the material, the lower the von mises stress, the lower the displacement and the higher safety factor. Tubes with a thickness of 0.5mm have a von mises stress of 4.43 MPa, a displacement of 4.7 x 10^{-4} mm with SF 56.4 is safe and were chosen because of the lowest material costs (IDR 360,009). The frame size was chosen 40x40x3 mm based on the SF frame value (26) with the lowest material cost (IDR 197,800). The shaft holder is also chosen for the size of 40x40x3mm where the SF value (3834) and the lowest material cost (IDR 14,400). Helical screw shaft size is chosen at 0.5mm thickness where SF is 304 and material costs IDR 100,968. The overall results of the static structural analysis on various sizes of the paper pulper machine components showed σ_{von} under σ_{yield}, small displacement, and SF is safe.

1. Introduction

The implementation of 5R (Reuse, Reduce, Recycle, Replace, Replant) is a solution for paper waste management efforts in Indonesia. Recycle activities are carried out by processing paper waste into paper pulp as art paper, new paper material, or packaging paper material. This paper waste recycling is in line with Law of the Republic of Indonesia Number 18 Year 2008 Article 1, which states that waste management can be carried out by reusing and recycling waste [1].

Paper recycling activities require a paper pulper machine to turn waste paper into pulp before it is used into new paper. Many small and medium enterprises (SMEs) in processing waste paper in Indonesia are constrained by the fact that pulper machines sold in the market have large-capacity industrial specifications, so the prices are expensive.

Paper pulper machines for small and medium businesses must have the capacity as needed and have an affordable price. The pulp machine designed by the Department of Mechanical Engineering

UNNES has a capacity according to the needs of SMEs, namely 83 litres/process. In order for the machine to have a low price, the components of a pulp machine must be made of safe to operate and cheap materials. To find out whether the pulp machine component design is safe, it is necessary to know the value of stress, displacement and safety factor using the finite element method. The Finite Element Method (FEM) is a powerful discretization technique that uses general unstructured grids to approximate the solutions of many partial differential equations (PDEs) [2]. Finite element method used to verify the design carried out [3]. One of the software that can be used for analysis using FEM is Catia. Catia offers solutions for the design of shapes, styles, surface workflows and visualizations to create, modify and validate complex innovative shapes [4]. There are many studies on the finite element method in design to determine the value of stress and displacement using FEM [2-10] [13-15]. None of the studies evaluated the components of a design that is safe using FEM and inexpensive based on material cost analysis. This paper deal with static structural analysis of pulp machine components of various sizes is analysed using the static structural analysis to determine the stress, displacement, and safety factor so that it is known whether the components are safe to use. The cost of material size variation is calculated to be selected for cheap but safe materials to use.

1.1. *Design of paper pulper machine*

The design of paper pulper machine has a production capacity of 83 liters/process. The design of the paper pulper machine includes: (1) main frame with 900 mm of length, 600 mm of width and 1100 mm of height; (2) tubes with sizes 500 mm of diameter and 600 mm of thickness; (3) shaft holder; (4) helical screw shaft; (5) 1.5 HP electric motor; (6) bearing F207 20 mm of diameter and UCP204 25 mm of diameter; (7) The drive system uses a pulley-belt connection with 3:4 ratio.

The design as shown at figure 1. Production capacity of 83 litres is obtained from ¾ volume of tube diameter 50 cm and its height is 60 cm. The bottom tube has a conical frustum shape so that the flow motion can be axial upward. The stirring component uses radial and axial stirrer. Electric motor rotation (1452rpm) is reduced by ¾ to 1089rpm. Axial stirrer consists of 3 sharp angular helical screws that function as blades and push material down axially. The material is driven down toward by helical screw with a rotational speed of 3267rpm (3 times to 1089rpm). At the bottom of the tube, the material is cut by a rotary blade (total 8 blades) with a rotation speed of 8712 rpm (8 times to 1089rpm). Stirring and cutting materials using helical screw and rotary blade. The axial push down prevents the mixture of material and water from squirt out from the tube. The radial stirrer utilizes 3 baffles attached to the inner tube wall. The function of the baffle is to stir the material in the radial direction and reduce the swirling and vortex motion in the tube. The design of the paper pulper machine is shown in figure 1. The parts list of paper pulper machine is presented in table 1.

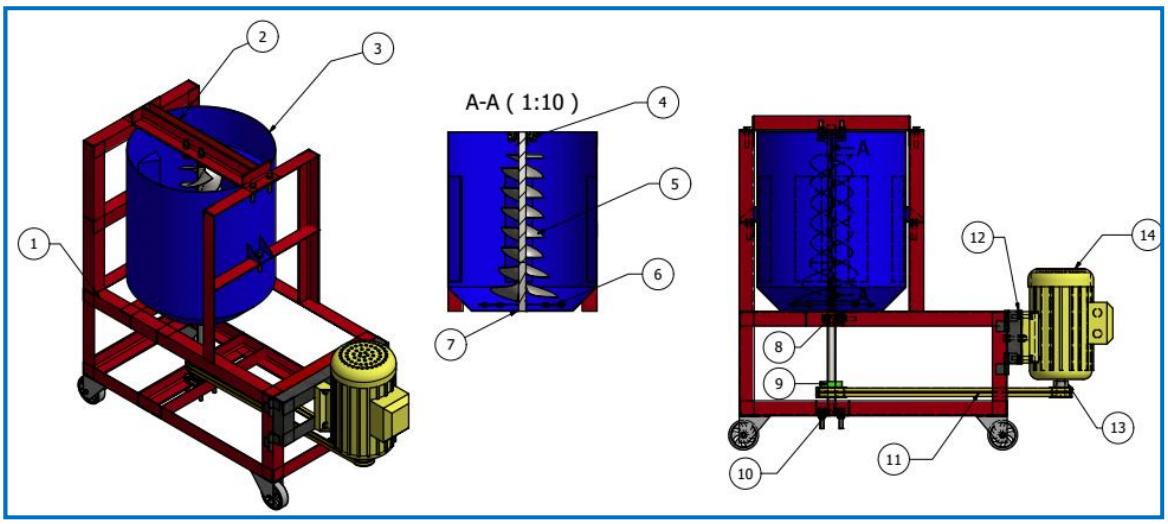

Figure 1. Design of Paper Pulper Machine (a) Isometric view (b) Left view

Table 1. Part list of Paper Pulper Machine

No	Part Name	No	Part Name	No	Part Name
1.	Main frame	6.	Rotary blade	11.	V-belt
2.	Shaft holder	7.	Rubber seal	12.	Electrical motor frame
3.	Pulper tube	8.	Bearing ucp204	13.	Driver pulley
4.	Bearing F207	9.	Driven pulley	14.	Electrical motor
5.	Helical screw shaft	10.	Bearing f207		

2. Method

Method in this study use simulation with finite element method. Strength analysis problem of pulper paper machine be solved with simulation of finite element method (FEM). FEM is a numeric technique for finding approximate solutions of partial differential equations (PDE) as well as of integral equations [6]. FEM simulation software used is CATIA V5R19. CATIA is as multiplatform CAD/CAM/CAE software suite developed by the modelling software company. This software helps in the creation of the geometry very accurately with the friendly-user commands for the better model [7].

Paper pulper machine as shown on figure 1 consists 14 components, but only 4 components were analysed in this study. The components analysed are pulper tube, main frame, shaft holder, and helical screw shaft. Finite Element Analysis uses CATIA V5R19 to calculate the von mises stress and translational displacement of 4 main part. Preprocessing of model of consist meshing, selection of material properties, selection clamp, and creation of load [8].

Cost evaluation is done by comparing the results of the calculation of the material cost for each variation. The lowest material cost is the criteria for selecting the materials used. The material costs (c) of the pulper tube is calculated from the size of the material multiplied by the material price per sheet.

Table 2. Material cost of SUS 304 and L shape ASTM A36

SUS 304		ASTM A36	
Thickness [mm]	**Price/sheet [IDR]***	**Thickness [mm]**	**Price/bar [IDR]****
0.5	551,737	40x40x3	86,000
0.6	662,085	40x40x4	111,000
0.8	882,780	40x40x5	141,000
1.0	1,103,475	50x50x3	127,000
1,5	1,655,212	50x50x4	142,020
2.0	2,206,949	50x50x5	186,440

(Sources: * PT. Citra Anggun Lestari, Jakarta Selatan, **PT. Tiga Baraya Jaya, Bogor, Jawa Barat. http://www.pusatbesibaja.co.id/harga-besi-siku-profil-baja-distributor-pabrik-supplier-agen-jual-toko-produsen/)

2.1. *Applications of material properties*

The mechanical properties of simulated materials were an important input data to the computational simulations [9]. The relevant property of each material is found within each element. Material properties such as young's modulus and Poisson's ratio can be utilized by computer generated analysis to describe the mechanical behaviour, induced stresses, or the relationship between forces and displacements for a structural element [10].

The main frame and shaft holder use angle bar material SNI 07-2054-2006 equivalent to JIS G3101 SS400 or ASTM A36. The tube and helical screw shaft use an ASTM A240 Grade 304 material. Material properties of paper pulper machine part is presented in table 3. Pulper tube and helical screw shaft use ASTM A240 Grade 304 material which is corrosion resistant. The corrosion-resistant material selected for the work process using a water. Each of part model of the paper pulper machine adjusted to the data material properties on table 3.

Table 3. Material properties of paper pulper machine part [11-12].

Part	Material	ρ [kg/m^3][a]	v [b]	σ_y[MPa][c]	E [GPa] [d]
Pulper tube	ASTM A240 Grade 304	7900	0.3	205	193
Main Frame	ASTM A36	7850	0.26	245	200
Shaft holder	ASTM A36	7850	0.26	245	200
Helical screw shaft	ASTM A240 Grade 304	7900	0.3	205	193

[a] the density
[b] the poissons ratio
[c] the yield strength of material
[d] the modulus of elasticity.

2.2. *Application of mesh*
Mesh size of each component is shown on table 4.

Table 4. Mesh size of pulper machine component

Part	Size		
	Absolute [mm]	No. of Element	No. of Nodes
Pulper tube	6.2	7730	2534
Main Frame	5.1	33819	10060
Shaft holder	6	2297	909
Helical screw shaft	9	3231	1280

2.3. *Loads and boundary condition*

2.3.1. Loads on pulper tube
The design of a pulper tube is shown in figure 2. Pulper tube specifications and the loads are presented in table 4. The weight of the tube contents is calculated by 3/4 volume times water density. Calculation of loads on pulper tube use an Equation 1 to 11.

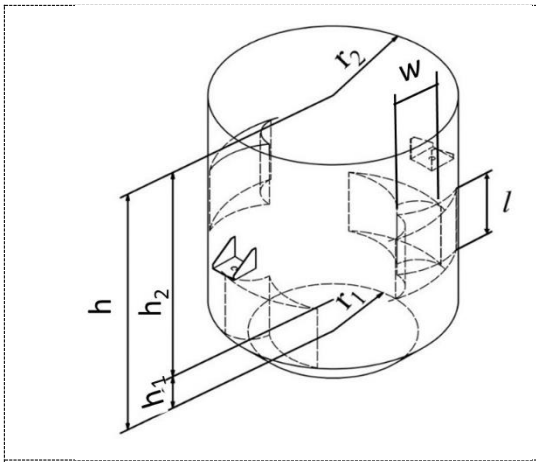

Figure 2. Design and geometry of pulper tube

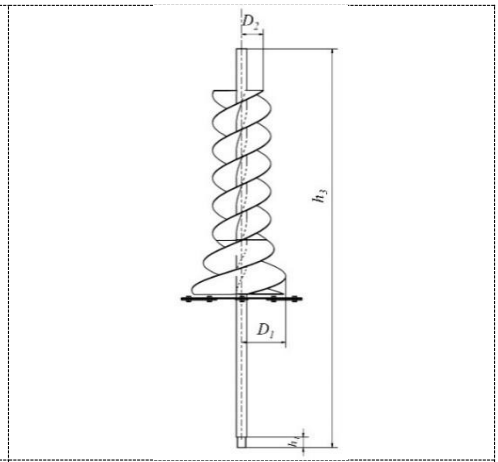

Figure 3. Design and geometry of helical screw shaft

$$V_{t1} = \pi \ {r_1}^2 \ h \tag{1}$$

$$V_{t2} = (\pi \ {r_2}^2 h_1) + \frac{1}{3}\pi \ h_2({r_2}^2 + \ r_1 r_2 + {r_1}^2) - V_{t1} \tag{2}$$

$$W_{t1} = \rho_w V_{t1} \ g \tag{3}$$

$$W_{t2} = \rho_w V_{t2}\, g \quad (4)$$

$$n_s = \frac{d_1}{d_2} n_m \quad (5)$$

$$\tau = \frac{P \text{ x } 60}{2\,\pi\, n_s} \quad (6)$$

$$F = \frac{\tau}{r_2} \quad (7)$$

$$\omega = \frac{2\,\pi\, n_s}{60} \quad (8)$$

$$\vec{v} = r_2\, \omega \quad (9)$$

$$p = \frac{F}{A} \quad (10)$$

$$A = l\ x\ w \quad (11)$$

Table 5. Pulper tube specifications and loads.

	r_1[m]	r_2[m]	h [m]	h_1 [m]	h_2 [m]	V_{t1} [m^3]	V_{t2} [m^3]	ρ_w[kg/m^3]	W_{t1} [N]	W_{t2} [N]	d_1 [m]	d_2[m]
Size	0.17	0.25	0.45	0.37	0.08	0.0408	0.043	1000	400.96	422.1	0.077	0.102
	n_m [rpm]	n_s [rpm]	P (watt)	τ [Nm]	ω [rad/s]	$\vec{v}$[m/s]	F [N]	l [m]	w [m]	A	p [N/m^2]	
size	1452	1089	1119	9.81	114.09	28.52	39.23	0.12	0.15	0.02	2326.3	

Where $r_1$the radius of conical frustum, r_2 the radius of tube, h the high of tube, h_1 the high of conical frustum, h_2 the high of contents maximum, V_{t1} the volume of tube centre, $V_{t2}$the volume of tube side, ρ_w the density of water, g the gravity, W_{t1} the load on tube base, W_{t2} the load on the sloping side of tube base, d_1 the diameter of driver pulley, d_2 the diameter of driven pulley, n_m the rotational speed of electrical motor, n_s the Rotational speed of helical screw, P the power of electrical motor, τ the effective torque of motor, ω the angular velocity, v the linear velocity, A the area subjected to pressure, F the tangential force, l the length of baffle, w the width of baffle, p the pressure to the baffle.

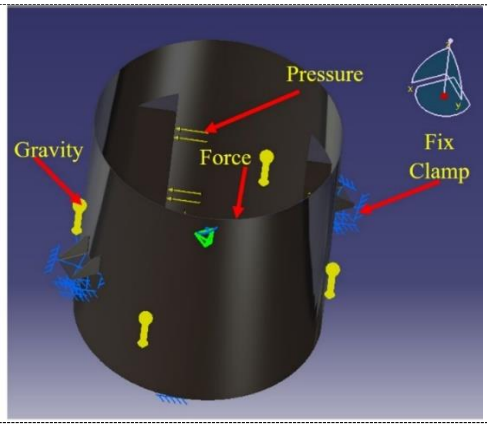

Figure 4. Loads and boundary condition of the pulper tube

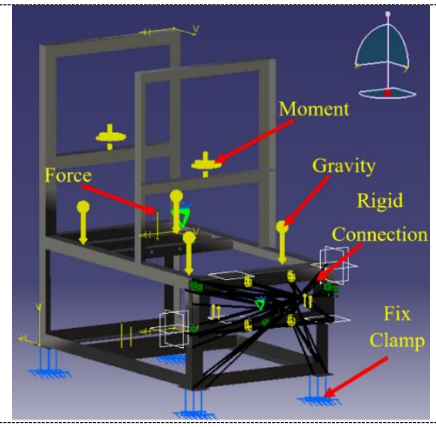

Figure 5. Loads and boundary condition of the main frame

The loads and boundary condition of the pulper tubes are shown in Figure 4. The load consists of pressure to the baffles (p) and forces to the base of conical frustum (W_{t1}+ W_{t2}). Gravity applied to the

pulper tube body and constraint (fix clamp) applied to the bottom of pulper tube, and bolt hole of stand pulper tube.

2.3.2. Loads of the main frame

The main frame gets a load of forces and moments. Force placed on the stand holder shaft (W_{hs}), stand pulper tube (W_{tb}), stand bearing of helical screw shaft (W_{bf}), and bolt hole of stand electrical motor (W_{em}). Moment applied to the tube holder (τ) and bolt hole (M_1) of stand electrical motor. The loads of the main frame are presented on Table 5. Gravity applied to the main frame body and constraint (fix clamp) applied to the bottom main frame. Application of loads of the shaft holder are shown on figure 5. Calculations of force and moment use equation 12 to 17.

$$W_{tb} = W_t + W_{t1} + W_{t2} \quad (12)$$

$$W_{sc} = W_{bs} + W_{sf1} + W_{sf2} \quad (13)$$

$$V_{sf1} = \frac{\pi}{4} {D_1}^2 h_3 \quad (14)$$

$$V_{sf2} = \frac{\pi}{4} {D_2}^2 h_3 \quad (15)$$

$$W_{sf1} = V_{sf1} \rho_{ss}\, g \quad (16)$$

$$W_{sf2} = V_{sf2} \rho_{ss}\, g \quad (17)$$

$$W_{bf} = W_{sc} + W_{bb1} + W_{f1+} W_{pl} \quad (18)$$

$$W_{pl} = W_{pl1} + W_{pl2} \quad (19)$$

Table 6. Loads of the main frame

	W_t [N]	W_{tb} [N]	D_1 [m]	D_2 [m]	V_{sf1}[m^3]	V_{sf2}[m^3]	ρ_{ss}[kg/m^3]	g[m/s^2]	W_{sf1}[N]	W_{sf2}[N]
Size	387.45	1210.52	0,025	0,02	4.69 x 10^4	7.86 x 10^6	7850	9.81	36.1	0.61
	W_{bs} [N]	**W_{sc} [N]**	**W_{bb1} [N]**	**W_{f1}[N]**	**W_{pl1}[N]**	**W_{pl2}[N]**	**W_{pl}[N]**	**W_{em} [N]**	**W_{bf}[N]**	**M_1[Nm]**
Size	14.98	51.7	5.42	0.52	13.56	9.56	23.12	290	80.76	29

Where $W_t$the weight of pulper tube, W_{tb} the total weight of the tube with its contents, $D_1$the large diameter shaft, D_2 the small diameter shaft, V_{sf1} the volume of D_1shaft, V_{sf2} the volume of D_2shaft, W_{sf1} the weight of D_1 shaft, Wsf_2 the weight of D_2 shaft, Wsc the weight of helical screw and rotary blade, $W_{f1}$the weight of fasteners, W_{bb1} the weight of bearing F207, W_{hs} the weight of holder shaft, W_{bb2} the weight of bearing UCP 204, W_{pl1} the weight of driven pulley, W_{bf} the loads of bottom frame, W_{em} the weight of electrical motor, W_{pl2} the weight of driver pulley, M_1 the moment of electrical motor weight.

2.3.3. Loads of the shaft holder.

Loads of the shaft holder consist of effective torque of motor, weight of fasteners, and weight of bearing. The fasteners and bearing weight are obtained by weighing the mass using scales. The loads of the shaft holder are presented on table 6. Application of loads to the shaft holder is shown in figure 6.

Table 7. Loads of the holder shaft

	τ [Nm]	W_{f1}[N]	W_{bb1}[N]	F_{tot} [N]
Size	9.81	0.52	5.42	5.94

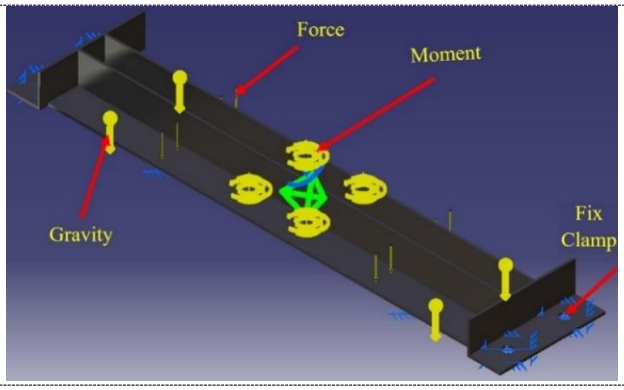

Figure 6. Loads and constraint of the holder shaft

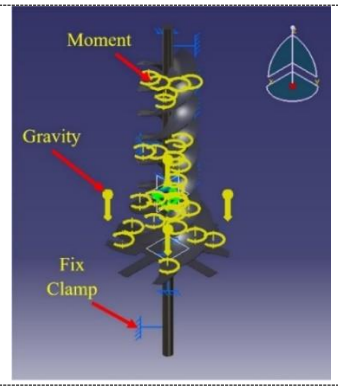

Figure 7. Loads and constraint of the helical screw shaft

Figure 6 show the application of force ($\boldsymbol{F_{tot}}$) to the bottom of 2 member of holder shaft, moment (torque "$\boldsymbol{\tau}$") to the 4 bolts hole, and gravity applied to the shaft holder body. Where *Ftot* the total weight of W_{bb1} added with$W_{fl.}$ The constraint on the shaft holder is placed in 4 bolt holes at the end of shaft holder and on the bottom surface. Constraint with the type of fix clamp.

2.3.4. Loads of the helical screw shaft.

Helical screw shaft only received a moment from the effective electrical motor (torque "τ") and constraint is placed to the shaft. The loads and boundary condition of helical Screw shaft are shown at figure 7.

3. Results and Discussion

3.1. *Determination of pulper tube material.*

FEM simulations on pulper tube models with thickness variations: 0.5; 0.6; 0.8; 1; 1.5; and 2 (mm). The results of von mises stress ($\boldsymbol{\sigma_{von}}$), deformation ($\boldsymbol{\delta}$), safety factor (SF) and cost (IDR) are shown in table 8. Plot von mises stress vs thickness variation show on Figure 8.

Von Mises stress is an adequate scalar measure of complex stress fields for ductile materials [13]. Safety factor value was varied and the results of FEA i.e. maximum stress were then compared to the yield strength value. Safety factor from analysis which results in close but not exceeding the yield strength values was selected [14]. Safety factor consider the semi-probabilistic safety format based on limit states with partial safetyfactors applied to the loads and the material strengths [15]. Safety factor of the pulper calculated by equation:

$$SF = \frac{\sigma_{yield}}{\sigma_{design}} \tag{20}$$

The safety factor of each component of the pulper machine following rules FoS = 2.0 to 2.5, for the design of machine elements that withstand dynamic loads with average confidence level for all design data [16]

Table 8. The von mises stress, safety factor, displacement and cost of pulper tube

Code	Size [mm]	σ_{von}[MPa]	*SF*	δ [mm]	*c* [IDR]
Tb1	0.5	4.43	56.4	0.00047	368,009
Tb2	0.6	0.870	287.3	0.00043	441,611
Tb3	0.8	0.742	336.9	0.000399	588,814
Tb4	1.0	0.652	383	0.000255	736,018
Tb5	1.5	0.393	636	0.000235	1,104,026
Tb6	2.0	0.347	720	0.000234	1,472,035

Table 8 also presents the material cost for each tube thickness variation. The largest of von mises stress at 0.5 mm tube thickness (4.43 MPa) and the smallest von mises stress at 2mm of thickness (0.347 MPa). Safety factor at 0.5 mm tube thickness reaches 56.4, so the design is safe. All variations in tube thickness have a safety factor of more than 2.5, so that the whole is declared safe. Material selection is based on the lowest C value, namely 0.5mm tube thickness with C value (IDR.368,009). The results value of this material cost is obtained from the required area of the tube plate of 1.92 m^2 from 2.88 m^2 or 66.7% of the plate sheet size 1.2 m x 2.4 m.

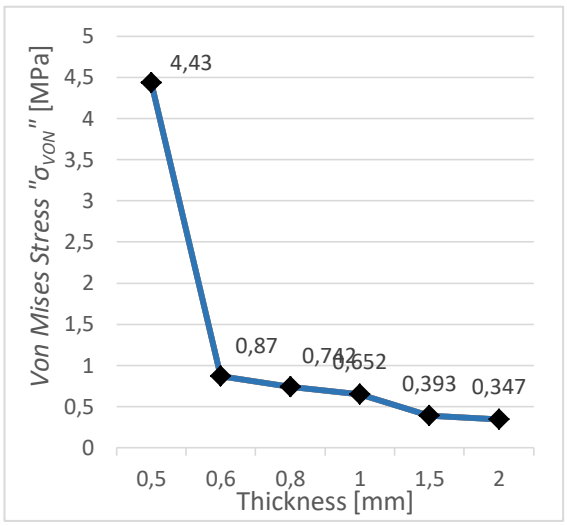

Figure 8. Plot stress vs thickness of tube

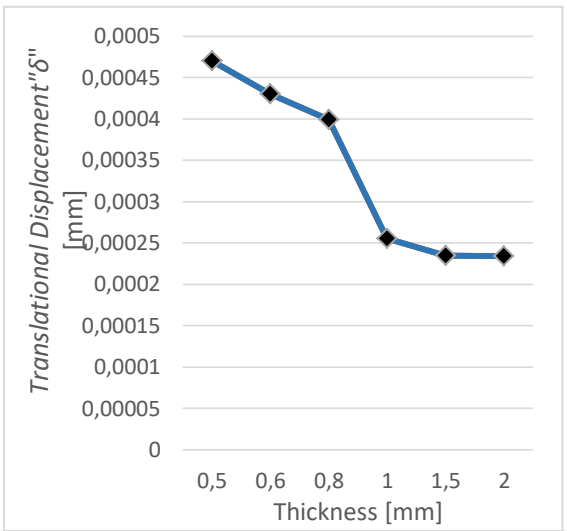

Figure 9. Plot displacement vs thickness of tube

The von mises stress of the variation in tube thickness has decreased significantly by 80%, from 04.43MPa (0.5mm thickness) to 0.87MPa (0.6mm thickness). Displacement has decreased with increasing thickness of the tube material (see Figure 9). The largest displacement value is 4.7 x 10^{-4}mm.

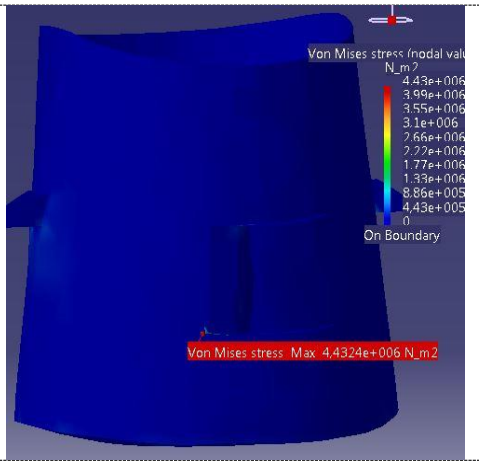

Figure 10. The maximum stress of tube with 0.5mm of thickness

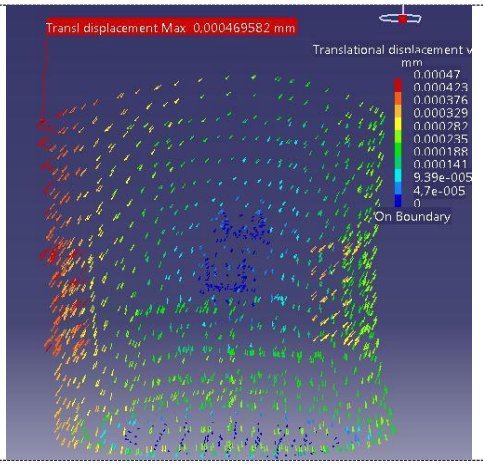

Figure 11. The maximum displacement of tube with 0.5mm of thickness

Figure 10 shows the largest von mises stress of 0.5mm of thickness at the stand tube connection with the tube wall. The red area indicates the maximum stress and the blue area is the minimum stress. Figure 11 shows the area with the largest displacement value of $4.7x10^{-4}$mm on the red vector.

3.2. *Determination of the main frame material.*

FEM simulations of the main frame with angle bar size variation. The results of von mises stress (**σ_{von}**), displacement (**δ**), safety factor (SF) and cost (c) of the main frame are shown in table 9. Plot von mises stress vs angle bar size is show on Figure 12. Plot displacement vs angle bar size is show on Figure 13.

Table 9. The von mises stress, safety factor, displacement and cost of the main frame

Code	Size [mm]	σ_{von}[MPa]	*SF*	δ [mm]	*C* [Rp]
FL1	40x40x3	9.29	26	0.0429	197,800
FL2	40x40x4	7.13	34	0.0413	255,300
FL3	40x40x5	7.05	35	0.0399	324,300
FL4	50x50x3	6.76	36	0.0254	292,100
FL5	50x50x4	4.79	51	0.0246	324,346
FL6	50x50x5	4.64	53	0.022	428,812

The largest von mises stress on FL1 main frame (9.29 MPa) and smallest von mises stress on FL6 main frame (4.64 MPa). The safety factor of the FL1 main frame (40x40x3mm) is 26, so the design is safe.

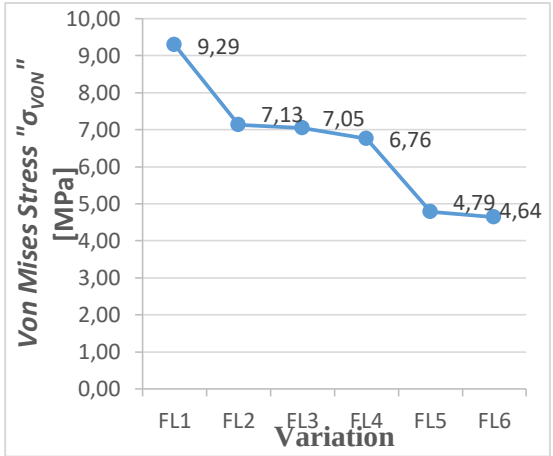

Figure 12. Plot stress vs variation of main frame

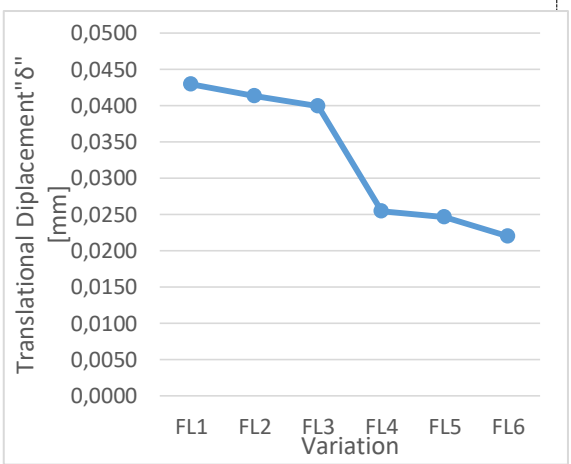

Figure 13. Plot displacement vs variation of main frame

The lowest safety factor of the main frame size variation is 26, so all variations are declared safe. The main frame material was selected with the FL1 code which has the lowest C value (IDR. 197,800). The results value of the material costmain frame are obtained from the length needed for l shape of 13.4 m or requires 2.3 bar of l shape.

Figure 12 indicates the von mises stress of variations angle bar size of the main frame showing a decrease. The largest decrease of stress (29%) from FL1 main frame (9.29 MPa) to FL2 (7.13 MPa). The largest decrease of displacement (23%) from FL3 main frame (0.0399mm) to FL4 (0.0254mm).

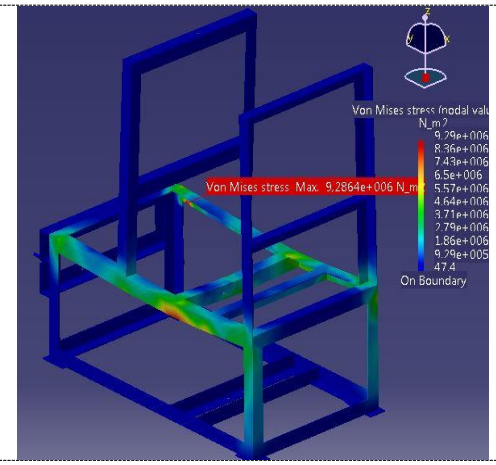

Figure 14. The maximum stress of FL1 main frame

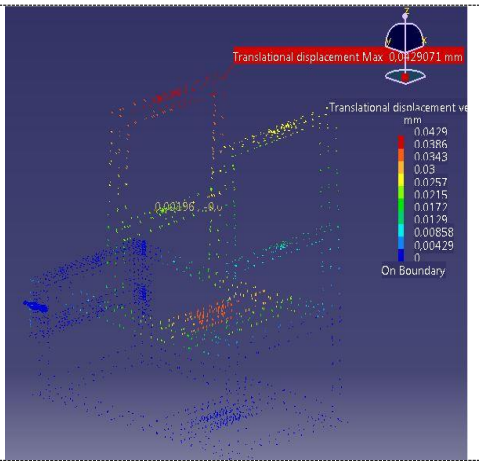

Figure 15. The maximum displacement of FL1 main frame

Figure 14 shows the largest von mises stress value on FL1 main frame (40 x 40 x 3 mm angle bar) of 9.29 MPa in the red area, which is the part that receives the bending load (longitudinal direction). Figure 15 shows the largest displacement value of 0.0429 mm on the stand shaft holder (red vector).

3.3. *Determination of the shaft holder material.*

FEM simulations results of the shaft holder with angle bar size variation are shown on Table 10. Plot von mises stress vs angle bar size is show on Figure 14. Plot displacement vs angle bar size is show on Figure 15.

Table 10. The von mises stress, safety factor, displacement and cost of shaft holder

Code	**Size [mm]**	σ_{von}**[MPa]**	***SF***	δ **[mm]**	***c*** **[IDR]**
HL1	40x40x3	0.064	3834	1.58E-06	14,400
HL2	40x40x4	0.061	4001	1.52E-06	18,500
HL3	40x40x5	0.053	4608	1.7E-06	23,500
HL4	50x50x3	0.045	8420	1.2E-06	21,200
HL5	50x50x4	0.034	8697	8E-07	23,600
HL6	50x50x5	0.015	15039	5.18E-07	31,100

The largest of von mises stress on HL1 shaft holder (0.064 MPa) and the smallest von mises stress on HL6 shaft holder (0.015 MPa). The safety factor of the HL1 shaft holder (40x40x3mm angle bar) is 3834, so the design is safe. The safety factor is very high caused this part only accepts a torque from the helical screw shaft. Based on table 10, all components are safe, so the selection of components is based on the lowest C value (IDR14,400). The results of the value material costs of the shaft holder are obtained from the length needed for l shape of 1.26 m or requires 0.21 bar of l shape.

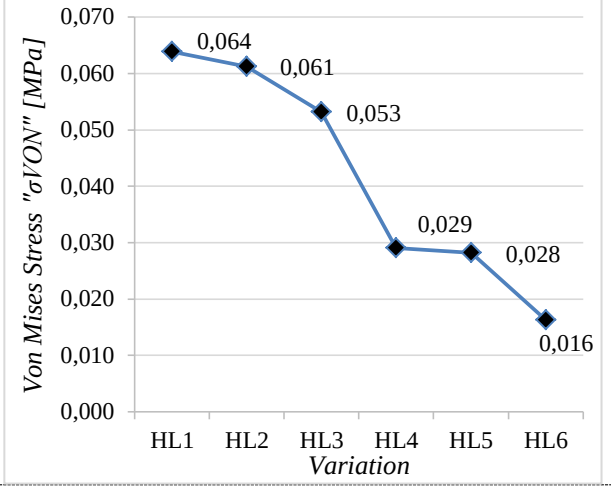

Figure 16. Plot stress vs thickness of holder

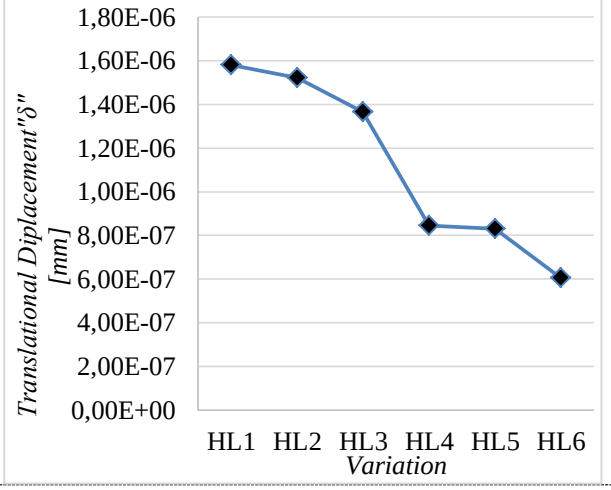

Figure 17. Plot displacement vs thickness of holder

Figure 16 shows the value of von mises stress decreases with the increasing angle bar size. The greatest reduction in stress (45%) in variations HL3 (0.053 MPa) to HL4 (0.029MPa). The largest decrease of displacement (38%) from HL3 variations ($1.37x10^{6}$mm) to HL4 ($8.4x\ 10^{7}$mm).

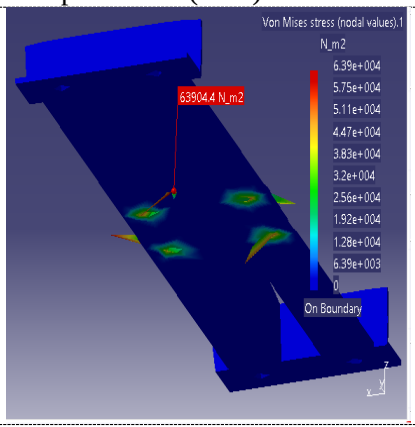

Figure 18. The maximum stress of HL1 variation

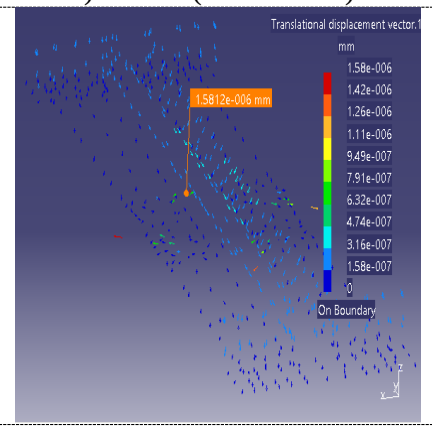

Figure 19. The maximum displacement of HL1 variation

3.4. Determination of the of the helical screw shaft material.
FEM simulations results of the shaft holder with angle bar size variation are shown on Table 11.

Table 11. The von mises stress, safety factor, displacement and cost of helical screw shaft

Code	Thickness [mm]	σ_{von}[MPa]	*SF*	δ [mm]	*C*[IDR]
Hs1	0.5	0.82	304	0.00075	100,968
Hs2	0.6	0.62	403	0.00067	121,162
Hs3	0.8	0.55	454	0.00063	161,549
Hs4	1	0.49	415	0.00059	201, 936
Hs5	1.5	0.39	576	0.00056	302,904
Hs6	2	0.35	647	0.00051	403,872

The largest of von mises stress (0.82 MPa) on 0.5mm thick screws and the smallest stress (0.35 MPa) on 2 mm thick screws. The safety factor of the helical screw shaft (0.5 mm) is 304, so the design is safe. Based on table 10, all variations of the helical screw shaft are safe, so the selection of component that uses is based on the lowest C value (IDR100,968). The results of the value of this material price are obtained from the required area of the screws plate of 0.53 m^2 from 2.88 m^2 or 18.3% of the plate sheet size 1.2 m x 2.4 m.

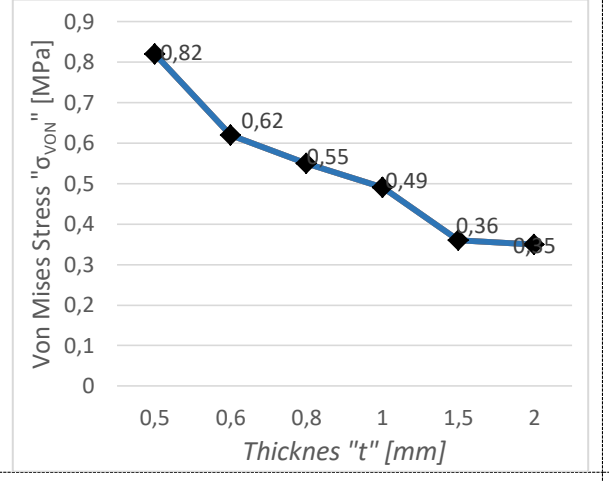

Figure 20. Plot stress vs thickness of helical screw

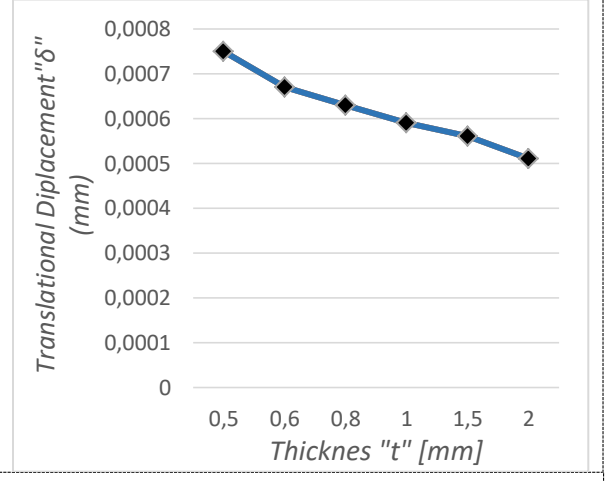

Figure 21. Plot displacement vs thickness of helical screw

The von mises stress decreases with thicker helical screw. The greatest decreases in stress (24,3%) from 0.5mm thick (0.82 MPa) to 0.6mm thick (0.62 MPa). The largest of displacement (12%) from variations in thickness of 0.5mm to 0.6mm.

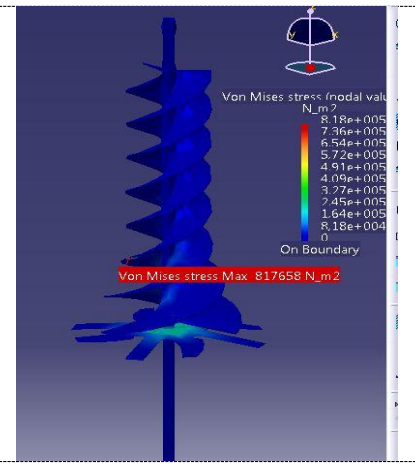

Figure 22. The maximum stress of 0.5mm thickness of the helical screw

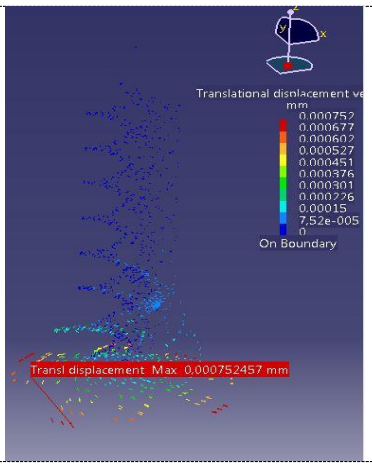

Figure 23. The maximum displacement of 0.5mm thickness of helical screw

Figure 22 shows the greatest von mises stress on a 0.5mm thick helical screw (0.82 MPa) on a rotary blade close to the shaft. Figure 23 shows the largest displacement value of 0.000752 mm at the tip of the rotary blade away from the support.

4. Conclusion

Based on the results of the study, it can be concluded that the von mises stress of each component of the paper waste pulper machine decreases as the thickness increases. Von mises stress that occurs of each variation of the pulper machine component is safe, because safety factor is more than 2.5.

Displacement produced on each component of the paper waste pulper machine has decreased from the increase in the thickness. All simulation results get a safety factor for each component more than 2.5 so that all designs are safe. Selection of material sizes for paper pulper machine components based on the lowest material cost. The material size of each components selected is a tube with a thickness of 0.5mm, main frame and shaft holder with a size of 40mm x 40mm x 3mm and a helical screw shaft with a thickness of 0.5mm.

References

[1] Anonymous 2008 *Undang-Undang Republik Indonesia Nomor 18 Tahun 2008 Pengelolaan Sampah Lembaran Negara Republik Indonesia Tahun 2008 Nomor 69* Jakarta
[2] Anderson R, Andrej J, Barker A, Bramwell J, Cerveny J S, Dobrev V, Dudouit Y, Fisher A, Kolev T, Pazner W, Stowell M, Tomov V, Akkerman I, Dahm J, Medina D, and Zampini S 2020 MFEM: A modular finite element methods library *Computers and Mathematics with Applications*
[3] Li L, Shen T, and Li Y K 2017 A Finite Element Analysis of Stress Distribution and Disk Displacement in Response to Lumbar Rotation Manipulation in the Sitting and Side-Lying Positions *Journal of Manipulative and Physiological Therapeutics* **40** 580-586
[4] Raju K V S, Raju G T, and Harsha N 2019 Modelling nad Structural Stress Analysis of Thrust Bearing *Materials Today Proceedings* **19** 2163-2171
[5] Moreno M F, Bertolino G, Yawny A 2016 The significance of specimen displacement definition on the mechanical properties derived from Small Punch Test *Materials and Design* **95** 623–663
[6] Chandru B T and Suresh P M 2017 Finite Element and Experimental Modal Analysis of Car Roof with and without Damper *Materials Today Proceedings* **4** 11237-11244
[7] Jun L, Wei Y, Yugang Z, Yang P, Yunsong R, and Wei W 2013 *Chinese Journal of Aeronautics* **26** 334-342
[8] Babu A V H, and Prasad B D 2019 Design and Analysis of Pinion and Crown for the Differential *Materials Today Proceedings* **16** 295-301
[9] Moreira T M M, Godefroid L B, Faria G L D, and Silveira R A D M 2019 Computational Analysis Via FEM Of Tirefond Screws Used In The Fastening System Of Railroads Aiming To Avoid A Recurrent Failure Case *Engineering Failure* Analysis **106** 1-12
[10] Lakshmi R D, Abraham A, Sekar V, and Hariharan A 2015 Influence Of Connector Dimensions On The Stress Distribution Of Monolithic Zirconia And Lithium-Di-Silicate Inlay Retained Fixed Dental Prostheses E A 3D Finite Element Analysis *Tanta Dental Journal* **12** 56-64
[11] Anonymous 2005 *Standard Specification for Carbon Structural Steel A36/36M-05* (West Conshohocken, PA: ASTM International)
[12] Anonymous 2013 *Stainless Steel Grade Datasheets* http://www.atlassteels.com.au/documents/Atlas_Grade_datasheet_304_rev_Jan_2011.pdf
[13] Fuente E D L 2009 Von Mises stresses in random vibration of linear structures *Computers and Structures* **87** 1253–1262
[14] Noor M A M, Rashid H, Mahyuddin W M F W, Azlan M A M, and Mahmud J 2012 Stress Analysis of a Low Loader Chasis, *Proceeding Engineering* **41** 995-1001
[15] Cugat V, Cavalaro S H P, Bairan J M, Fuente A D L 2020 Safety Format For Theflexural Design Of Tunnelfibre Reinforced Concreteprecast Segmental Linings *Tunnelling and Underground Space Technology* **103** 1-8
[16] Mott R L 1985 *Machine Element in Mechanical Design* (Singapore: Prentice Hall)